Influence of Modes of Climate Variability on Global Precipitation Extremes

Influence of Modes of Climate Variability on Global Precipitation Extremes

JESSE KENYON

Nicholas School for the Environment and Earth Sciences, Duke University, Durham, North Carolina

GABRIELE C. HEGERL

School of GeoSciences, The University of Edinburgh, Edinburgh, United Kingdom

(Manuscript received 13 January 2010, in final form 24 June 2010)

ABSTRACT

The probability of climate extremes is strongly affected by atmospheric circulation. This study quantifies the worldwide influence of three major modes of circulation on station-based indices of intense precipitation: the El Niño–Southern Oscillation, the Pacific interdecadal variability as characterized by the North Pacific index (NPI), and the North Atlantic Oscillation–Northern Annular Mode. The study examines which stations show a statistically significant (5%) difference between the positive and negative phases of a circulation regime. Results show distinct regional patterns of response to all these modes of climate variability; however, precipitation extremes are most substantially affected by the El Niño–Southern Oscillation. The effects of the El Niño–Southern Oscillation are seen throughout the world, including in India, Africa, South America, the Pacific Rim, North America, and, weakly, Europe. The North Atlantic Oscillation has a strong, continent-wide effect on Eurasia and affects a small, but not negligible, percentage of stations across the Northern Hemispheric midlatitudes. This percentage increases slightly if the Northern Annular Mode index is used rather than the NAO index. In that case, a region of increase in intense precipitation can also be found in Southeast Asia. The NPI influence on precipitation extremes is similar to the response to El Niño, and strongest in landmasses adjacent to the Pacific. Consistently, indices of more rare precipitation events show a weaker response to circulation than indices of moderate extremes; the results are quite similar, but of opposite sign, for negative anomalies of the circulation indices.

1. Introduction

The variation of total or average precipitation with major modes of atmospheric circulation has been described and analyzed thoroughly in the scientific literature. For example, it has been known since Bjerknes that El Niño affects precipitation (Rasmusson and Wallace 1983). Southeast Asia, Indonesia, and Australia become drier during an El Niño as the tropical rainfall pattern shifts east (Rasmusson and Carpenter 1982; Rasmusson and Wallace 1983), meanwhile the southern tier of the United States from coast to coast becomes wetter during El Niño phases (Ropelewski and Halpert 1986). Positive events of the North Atlantic Oscillation (NAO) are generally associated with wetter conditions in northern Europe and drier conditions in southern Europe (see, e.g., Hurrell et al. 2003; Scaife et al. 2008). Deser et al. (2004) have explored the connection between precipitation and the North Pacific index (NPI), focusing on the tropics. They show that the NPI might be related to epochal changes in precipitation, with regions along the southern Pacific convergence zone being generally wetter during positive NPI phases. Power et al. (1999) studied how the interdecadal Pacific oscillation [IPO, which correlates to the NPI through interdecadal variations in tropical Pacific sea surface temperature (SST)] and the Southern Oscillation index (SOI) affect Australian rainfall. They find that when the IPO produces cooler sea surface temperatures (SST) in the tropical Pacific (positive NPI phase), this modulates how both phases of ENSO affect Australian rainfall. In contrast, IPO phases of warmer SSTs do not seem to have a strong impact on the response to either warm or cold ENSO phases.

Variations in global-scale extreme precipitation with circulation have been studied less intensely than changes

Corresponding author address: Gabriele C. Hegerl, School of GeoSciences, Grant Institute, The University of Edinburgh, The King's Buildings, West Mains Road, Edinburgh EH9 3JW, United Kingdom.
E-mail: gabi.hegerl@ed.ac.uk

DOI: 10.1175/2010JCLI3617.1

in mean or total precipitation, and studies usually focus on regions rather than analyzing worldwide data for extremes. However, extreme precipitation events are of great importance to society. They may cause flooding events, or conversely extreme precipitation may be the main mechanism for recharging reservoirs and watersheds. It has been pointed out (Thompson and Wallace 2001) that circulation regimes may strongly influence climate extremes, and a precursor study of the present study (Kenyon and Hegerl 2008) found worldwide and very strong influences of circulation on temperature extremes.

Few studies have analyzed the changes in global precipitation extremes with circulation. Alexander et al. (2009) used the method of self-organizing maps (SOMs) to diagnose global variations in indices of precipitation extremes caused by the El Niño–Southern Oscillation. The authors reduced sea surface temperature (SST) variability to eight patterns, of which the first pattern is a distinct La Niña while the eighth pattern is El Niño. The authors analyzed over which regions statistically significant differences occur in the values of the extreme precipitation indices between seasons with the La Niña SST pattern and seasons with the El Niño pattern. They found that during El Niño phases, Brazil, the southwestern United States, central Asia, and parts of China and New Zealand are wetter. Alexander et al. (2009) found a stronger signal with a detrended analysis, suggesting that anthropogenic climate change may have a confounding effect on the relationship of extreme precipitation to circulation, which may be partly due to a trend in their SOM pattern that relates to El Niño.

Allan and Soden (2008) have studied the global response of warm El Niño events on tropical precipitation in order to assess the response of climate models to greenhouse gas increases. They show that higher column water vapor is associated with warm El Niño events and this results in a greater percentage of anomalous heavy precipitation during El Niño than during the cold conditions of La Niña. They also demonstrate that light precipitation events more often occur in La Niña phases than El Niño phases. This links to other papers (Wentz et al. 2007; Soden et al. 2005) relating water vapor increases in the troposphere to increases in heavier precipitation.

Meehl et al. (2007) compared simulated and observed El Niño responses of extreme precipitation for North American winter (December–February, DJF), and found that El Niño winters have anomalously intensified wet extremes along the southern tier of the United States, the eastern coast, and the southwest. In contrast, precipitation intensity decreased in the Pacific Northwest and the Midwest. Zhang et al. (2010) has explored the connection between observed extreme precipitation over North America and the same three modes of climate variability that we explore, but focused on rarer precipitation extremes, namely return periods of the three independent days of largest precipitation amounts observed at stations. The authors used indices for El Niño, Pacific decadal variability, and the NAO as covariates in a study of changes in parameters of the generalized extreme value distribution (GEV) with circulation. The results showed that El Niño or Pacific decadal variability can lead to increased extreme precipitation in the southern tier of North America, but not the northern half of the continent. They also looked at how the PDO affects extreme precipitation via its influence on ENSO.

Power et al. (1999), Arblaster et al. (2002), Meehl and Hu (2006), and McGregor et al. (2007, 2008) have all analyzed interdecadal Pacific variability and how it modulates ENSO, using observations and models to tease out the mechanisms by which the variability occurs. In their model results, both Arblaster et al. (2002) and McGregor et al. (2007) found that the rising branch of the Walker circulation shifts eastward during the positive phase of the IPO (which is associated with interdecadal warmer SSTs in the eastern Pacific), diminishing the role of ENSO in its effects on Australian rainfall.

Meehl and Hu (2006) explored drought variability in the Indian monsoon region and the Great Basin region of the western United States in a 1360-yr run of a general circulation model (GCM). The authors find that during positive IPO phases (associated with warm tropical Pacific SST anomalies), the Indian monsoon region suffers a mega-drought (which they define as 20 consecutive years of negative area-averaged precipitation anomaly) while the Great Basin region is anomalously wet. In negative phases the two regions switch. Mechanisms involve wind-forced ocean Rossby waves affecting SSTs on a decadal time scale, and invoke atmosphere–ocean and tropical–midlatitudinal interactions.

For Europe and western Asia, the NAO has been shown to have a significant impact on weather extremes. Haylock and Goodess (2004) studied interannual variability of winter rainfall extremes over Europe and found a significant correspondence with the NAO. The authors analyzed both the number of days above the 1960–91's 90th percentile of wet-day amounts, and the maximum number of consecutive dry days over the period of 1958–2000 and found that, while local convective processes are important in summertime, a substantial fraction of the variability in extreme winter rainfall is associated with the NAO. The authors also found that the recent upward trend in the NAO is contributing to trends in extreme rainfall. Scaife et al. (2008) also looked at the effects of the NAO on winter extremes in Europe. They quantified the correlation between NAO and heavy winter rainfall for the whole

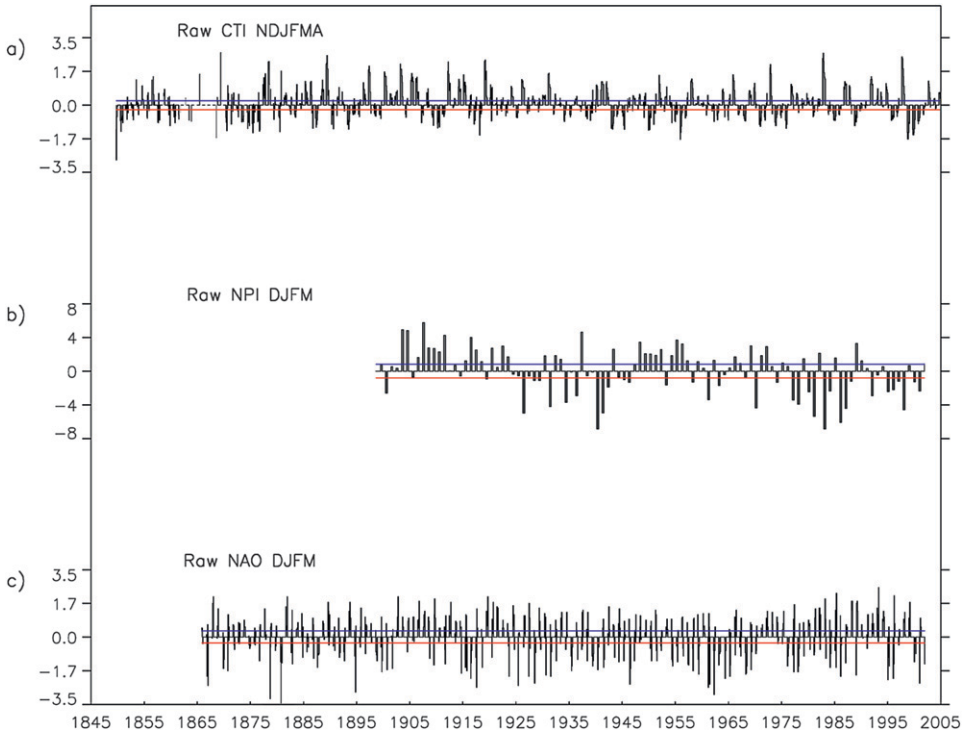

FIG. 1. Indices for large-scale circulations used in this paper: (a) the CTI of monthly SST anomalies for the 6°S–6°N Pacific equatorial region (°C); (b), the NPI, consisting of area-averaged SLP anomalies for the 4-month period DJFM (mb); and (c) the NAO index for the 4-month period DJFM (mb). The blue and red lines show the thresholds of 0.3 standard deviations for each index, which is used to determine positive and negative phases; periods in between are considered neutral.

twentieth century (1901–2000) and found a distinct dipole between northern and southern Europe. Their results show that southern Europe, especially the Iberian Peninsula, experiences much fewer rain events above the 90th percentile during high phases of the NAO, while southern Scandinavia has more rain events above 1961–90's 90th percentile.

The recent availability of the indices of climate extremes that were collected by the Expert Team on Climate Change Detection, and Indices (ETCCDI) offers the opportunity to compare variations in several indices of precipitation extremes between stations worldwide (Frich et al. 2002; Alexander et al. 2006). The motivation for the existence of ETCCDI climate indices and information on how climate data are collected is given in Peterson and Manton (2008).

The present paper is a follow-on to our publication on changes in temperature extremes with circulation (Kenyon and Hegerl 2008, hereafter KH08). In this paper, we explore how precipitation extremes of different rarities respond to circulation. We have also investigated the effects of a lagged relationship of intense precipitation to El Niño and the effects of the Southern Annular Mode on midlatitude precipitation extremes in the SH. Our analysis is performed on five climatic indices of extreme precipitation produced by ETCCDI. A discussion of these extremes indices, and their calculation, can be found in KH08 and Alexander et al. (2006), and more briefly in section 2 of this paper, which also introduces the circulation indices. Section 3 briefly describes the method of analysis. Results are presented in section 4, followed by conclusions in section 5.

2. Data

a. Circulation patterns

Here, we briefly describe the indices of the major climate modes used to analyze the effects of circulation on precipitation extremes. Full descriptions are available in our earlier paper on temperature extremes (KH08). For the El Niño–Southern Oscillation, we use the cold tongue index (CTI; see Fig. 1a) obtained from the Joint Institute for the Study of the Atmosphere and Ocean (JISAO) at the University of Washington (information online at jisao.washington.edu/data/cti/). The index is a measure of monthly SST anomalies (1849–2005) from 6°S to 6°N, spanning 180° to 90°W. Each monthly value is the average

anomaly for the 270 grid boxes covering 2° × 2° over this region, taken with respect to the 1950–79 climatology. In the previous paper, we compared results using that index with connections to Niño-3.4 and other El Niño indices, and found results that were quite robust between index choices.

We construct both an annual index and two 6-month seasonal indices for ENSO: May–October, for the boreal warm season, and November–April, for the boreal cold season (hereafter MJJASO and NDJFMA, respectively). The seasonal means of the CTI are compared against a threshold of 0.3 standard deviations of the CTI's monthly variability. If a season exceeds the positive threshold of 0.3 standard deviations, it is considered to be El Niño like, if it is less than −0.3 standard deviations, it is considered to be La Niña like. The value of 0.3 as a threshold was chosen as a compromise, ignoring seasons that are truly neutral while maintaining a large enough sample size for statistical robustness. Figure 1d in KH08 shows the CTI converted into a time series of on–off switches for each cold half-year. Figure 1a shows El Niño–La Niña phases based on the entire 1849–2005 CTI record, but in the subsequent analysis of precipitation extremes, we use only the subset of 1896–2004, which overlaps best with the prevailing station record lengths found in the extremes indices.

Pacific interdecadal variability is represented by the sea level pressure (SLP)-based NPI (Fig. 1b) rather than an SST-based index such as the PDO (for a discussion of Pacific indices, see KH08). The NPI is defined by Trenberth and Hurrell [(1994); see also Deser et al. (2004)] as the area-averaged, wintertime (DJFM) sea level pressure over the North Pacific region bounded by 30°–65°N and 140°E–160°W and, hence, is anticorrelated to the Pacific decadal oscillation (positive NPI anomalies are associated with cold SST anomalies in the eastern tropical Pacific, and warm anomalies over large parts of the North Pacific). The NPI used in this study spans the years 1899–2002, and the determination of positive, neutral, and negative phases was performed in the same manner as the CTI index.

Both the NPI and the CTI are Pacific based yet have a very small correlation over the overlapping period of 1899–2002, which is not surprising since they describe variability at different time scales. This makes it worthwhile to study the NPI separately. However, both the NPI and the CTI invoke circulation changes by similar mechanisms, since both have similar patterns of sea level pressure and sea surface temperature variability (see, e.g., the discussion in Zhang et al. 1997).

The third circulation mode explored is the North Atlantic Oscillation (NAO; see Fig. 1c). We use an NAO index that is defined as the normalized pressure difference between a station in the Azores (Ponte Delgada) and the Stykkisholmu station in Iceland (Hurrell and van Loon 1997; Hurrell et al. 2003), and that is available starting in January 1865. Again, a more detailed description of the construction is given in KH08. Since the large-scale dynamical effects of NAO and the NPI mainly manifest themselves in wintertime, we analyze the effects of these two circulations only for DJFM and only for the Northern Hemisphere. The NAO is strongly related to the Northern Annular Mode (NAM; Thompson and Wallace 1998; Thompson et al. 2000; see also Hurrell et al. 2003), which is a hemisphere-wide circulation pattern that extends from the troposphere to the stratosphere and is mirrored in the Southern Hemispheric Southern Annular Mode (see Gillett et al. 2006). We explore the relationship of precipitation extremes to both the Southern and Northern Annular Modes. A further key pattern of variability in the Northern Hemisphere is the Pacific–North America (PNA) pattern. This mode is one of the mechanisms by which El Niño events affect North American climate (see Hurrell et al. 2003) and thus is not studied directly in the present paper.

We showed in KH08 that connections between temperature extremes and circulation are quite insensitive to using different indices for the same circulation type (such as the NAM index rather than the NAO, the Pacific decadal oscillation index rather than the NPI, or Niño-4.3 rather than CTI), and that for those indices with trends (such as the NAO), detrending made very little difference to the results. For precipitation, we found nonnegligible, but small sensitivity to using the NAM rather than the NAO, which is illustrated below. Only results for the Southern Annular Mode were sensitive to subtracting the linear trend from the circulation index.

b. Indices of heavy precipitation

Station-based indices that determine the daily variability of temperature and precipitation have been collected by the ETCCDI. Some stations have indices going back to the late nineteenth century; however, coverage is much better during the second half of the twentieth century (see Alexander et al. 2006). Data coverage varies between very densely sampled regions (e.g., Europe, Asia, India, and the United States) and regions with much sparser coverage (such as northern Africa and South America, but excepting Argentina and southern Brazil). We focus our analysis on the index of the largest amount of daily precipitation over a single day, named RX1day, and the index of the largest five consecutive days of precipitation (RX5day). Data reliability and homogeneity issues are particularly critical for extreme events. However, for precipitation, measurements of very heavy events are generally more reliable than those of small events or counts of dry days (see, e.g., Groisman et al. 2005).

The RX indices (RX1day and RX5day) are available monthly, and extremes indices are calculated from daily data over a month, unless more than 3 days are missing (information online at http://cccma.seos.uvic.ca/ETCCDI/). Seasonal and annual ''extreme'' indices can be derived by either choosing the most extreme monthly index (such as the wettest event) from several months, or by averaging extremes indices. While the averaged months may in some locations be one of very few events available and thus be a quite ''normal'' event, the wettest 1- or 5-day event over a season will be more of an actual extreme event. We analyzed both averages and extremes of these indices at the annual and seasonal scales: a wintertime season (DJFM) for use with the two winter circulations of NAO and NPI, and a half-year mean for use with ENSO, consisting of the boreal cold season (NDJFMA) and the boreal warm season (MJJASO).

We also analyzed changes in an index of total precipitation (PRCPTOT) and in two percentile indices that describe the amount (mm) in the total, annual precipitation from days exceeding the climatological 99th and 95th percentiles of daily precipitation (R99P and R95P, respectively). These indices were available to us only as annual indices, and their percentile thresholds are calculated from the 1961–90 base period (see Alexander et al. 2006).

3. Methodology

The monthly precipitation extremes indices (RX1day and RX5day) are processed, either by averaging or by picking the most extreme monthly value, to arrive at cold and warm season extremes indices. In the case of the NAO and NPI, we require all four months of DJFM to be available for producing a seasonal mean. In the case of the CTI, four out of the six months are required to produce a half-season. Since stations usually report quite consistently through periods when they are active, these subjective choices make little difference to our results. Finally, we use only stations that have at least 30 yr of valid data (not necessarily consecutive), and the analysis is performed over the maximal length of overlap between each station-based index and the circulation indices (at most 1896–2002 for ENSO, 1899–2002 for the NPI analysis, and 1865–2002 for the NAO).

The circulation index (CTI, NPI, or NAO) is used as an on–off switch that selects seasons where the precipitation extremes coincide with a positive or negative circulation index. Those selected seasons are then analyzed to determine stations where the seasonal intensity of the index is significantly different between the positive and negative states of the circulation index. This analysis method thus avoids assumptions of linearity. However, both the results in KH08 and those reported here find only small and regional deviations from linearity. A regional deviation from linearity, for example, was found by Power et al. (2006), who point out that while an unusually strong La Niña can result in unusually strong Australian rainfall, a stronger than normal El Niño does not necessarily result in a particularly extreme precipitation deficit. For the present paper, we have analyzed the results in response to positive and negative circulation anomalies and, generally, found little visible deviation from linearity.

In the case of the annual-only indices (R99P, R95P, and PRCPTOT), an annual CTI index is used in the same fashion as the seasonal scale described above to analyze how increasingly rare events respond to circulation (note that we do not analyze the relationship to NPI and NAO, as those circulation modes are more appropriate for wintertime rather than annual analysis). Generally, increasingly rare events will be more affected by random sampling variability and changes will be noisier. In some instances the response of the heavy precipitation (e.g., to anthropogenic forcing) can be stronger and more regionally consistent than that of mean precipitation (see Hegerl et al. 2004). However, it will be shown below that this compensation does not appear to occur for the response of extreme precipitation to El Niño.

To determine if the different phases of a major circulation mode cause a significant difference in the values of the precipitation extremes indices for an individual station, we use a nonparametric Mann–Whitney test, as in KH08. We test the null hypothesis that the distribution of the precipitation extreme index during a positive circulation phase is no different from that during the negative circulation phase. This is done by calculating a sum of ranks of the events during positive and negative circulation anomalies. If the probability of obtaining a particular rank sum by chance is less than, or equal to, some significance level (we use 0.05), the null hypothesis is rejected, and we can say that, over the time period, seasons associated with the positive phase of the circulation at this station differ at a statistically significant level from seasons associated with the negative phase. More detail on this analysis method can be found in von Storch and Zwiers (1999) and in KH08.

The resulting significant stations are plotted in Figs. 2–6. Since some significant results among a large number of stations are expected from chance alone (on average 5% of stations for a 5% significance level), we also give the percentage of significant stations found in eight geographic regions in Tables 1–4 . We do not explicitly account for autocorrelation. However, the use of binary on–off switches, and the frequent transition between negative and positive states, even for the NPI (Fig. 1c), should make results quite insensitive to autocorrelation.

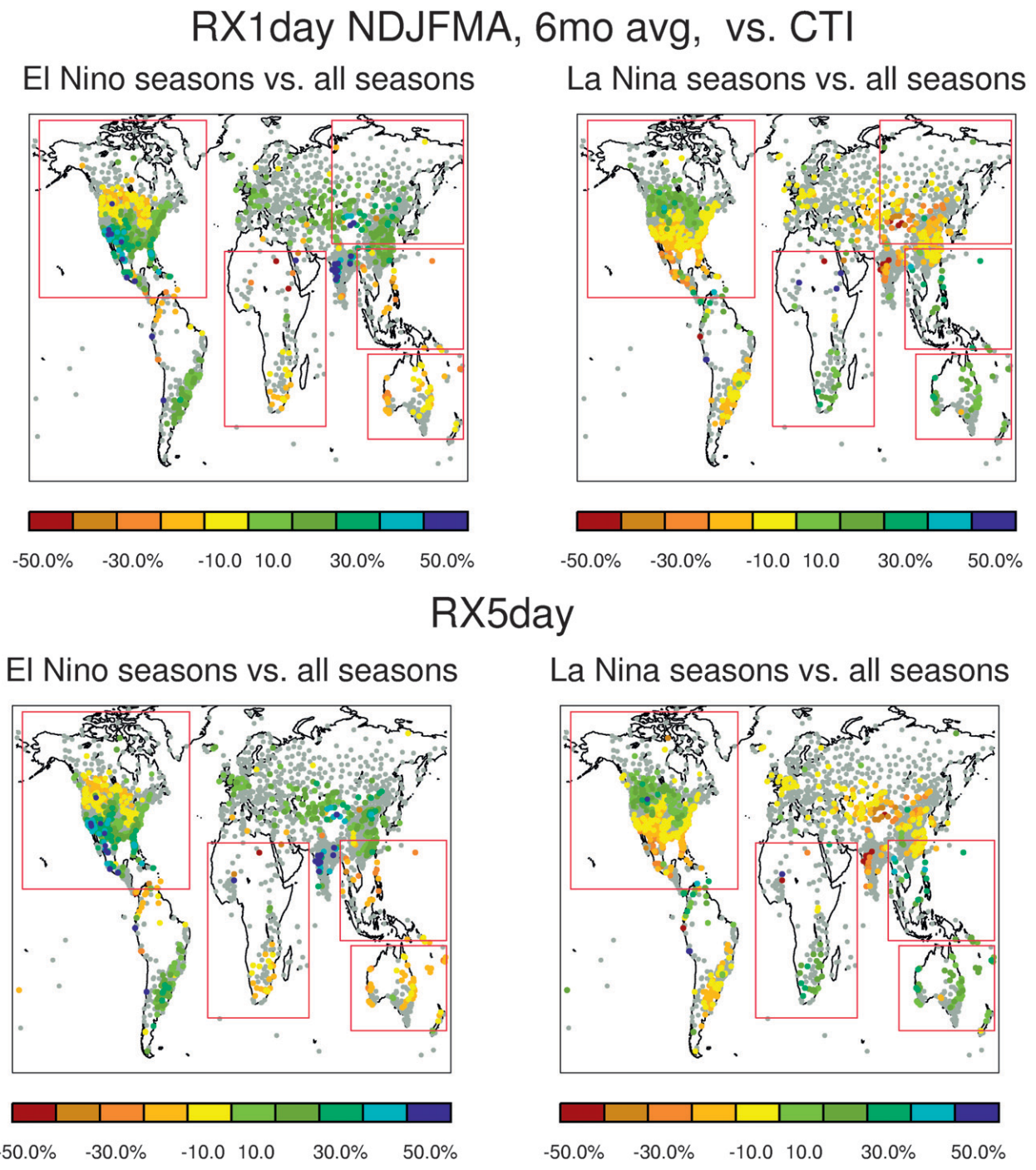

FIG. 2. Difference (%) of intense precipitation indices during (left) El Niño and (right) La Niña boreal cold season months (NDJFMA) compared to the average of all winter seasons. Indices are for RX1day (top row) and RX5day (bottom row). Red colors indicate decreased intense precipitation; blue colors indicate increases. Available stations that do not show a significant response are displayed as light gray dots. Red boxes outline continents where 25% or more of the stations responded significantly to ENSO phases. Regional boundaries are defined in Table 1. The southwest United States, Central America, and India all experience strong increases in extreme precipitation, while Australia, southern Africa, Southeast Asia, and the Pacific Northwest respond to El Niño phases with moderate to strongly moderate decreases in intense precipitation.

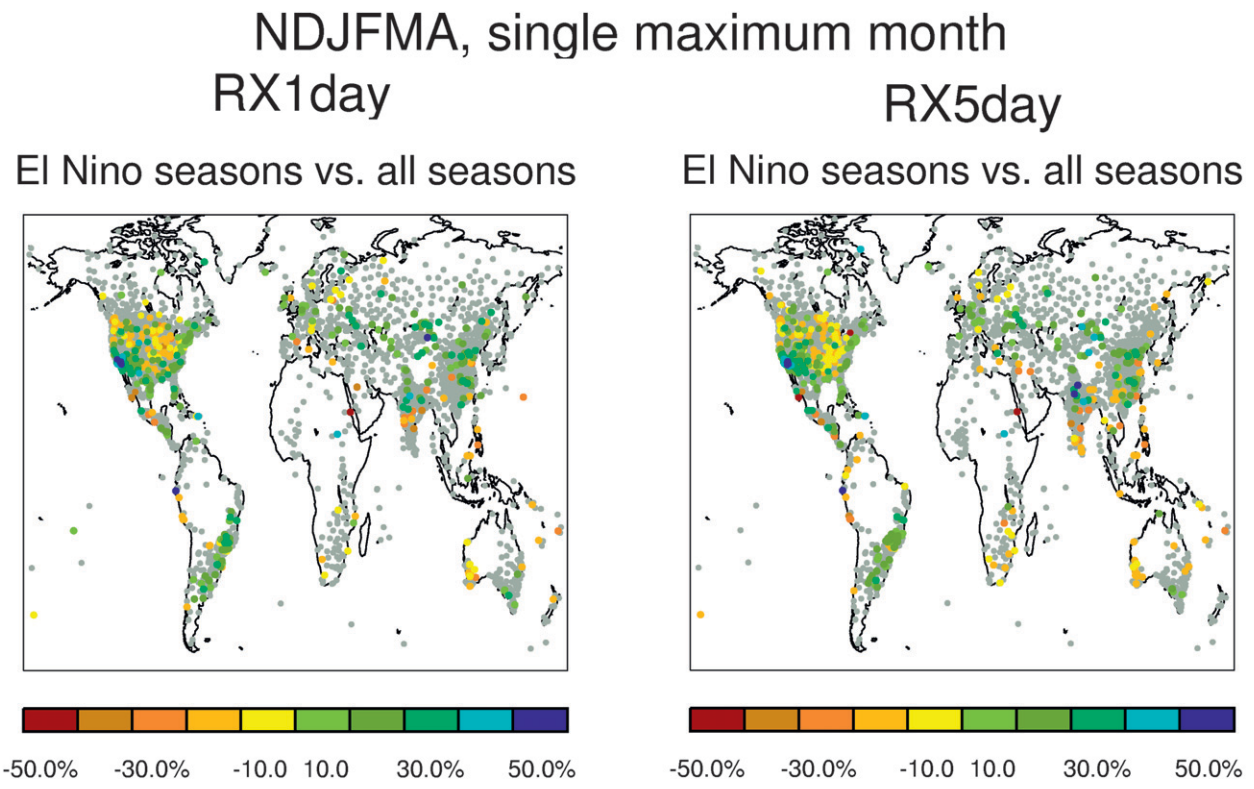

FIG. 3. As in the top row of Fig. 2, but showing the single wettest RX1day and RX5day events of the boreal cold season rather than an average of the monthly wet extremes. The response is similar to the averaged months shown in Fig. 2 but muted.

4. Results

The indices show a distinct response to each circulation regime, demonstrating that large circulation regimes affect extreme precipitation. A detailed examination of results for each, large-scale, circulation regime is discussed subsequently.

a. El Niño–La Niña

Table 1 shows the percentage of all stations, in eight broad geographic regions, that respond significantly (at the 5% level) to the circulation regimes both for the seasonal average response (averaging all monthly values) and the result of isolating just the single month with the maximum value for the season. The seasonal nature of ENSO is clearly seen (Table 1) in the difference between the response of a Northern Hemisphere region, such as North America, where many fewer stations respond in summer, and a Southern Hemisphere region, like Australia, that sees its greatest impact during the boreal summer. We experimented with applying lags to the connection with El Niño, since the atmospheric response can lag El Niño by several months (see, e.g., Hegerl and Wallace 2002). In the case of the boreal cold season, we used the NDJFMA indices of extremes in conjunction with CTI for the October–March season (1-month lead) or August–February season (3-month lead). The results of these lead–lag experiments are given in Table 1. In general, the number of significantly responding stations is within a couple of percentage points of each other between lagged and non-lagged cases, particularly for geographically close regions, such as Australia. However, in some regions that are distant from the equatorial Pacific, for instance Europe and Africa, the lagged responses are consistently stronger. An exception is South America, which shows by far the most significant response to a 3-month lag in the boreal summer season. This suggests that complex atmospheric teleconnections are at work whose delay relative to the ENSO forcing depends on the region and season. Since, otherwise, results are quite similar with and without lags, figures shown in this paper are based on instantaneous connections to the circulation.

We find that the patterns of extreme precipitation generally follow the patterns for mean precipitation described in the literature, with Southeast Asia, Indonesia, Australia, and the northern-most corner of South America showing reduced extreme precipitation during an El Niño, while the southern tier of the United States, from coast to coast, as well as Argentina–southern Brazil show increased heavy precipitation during El Niño phases. However, the

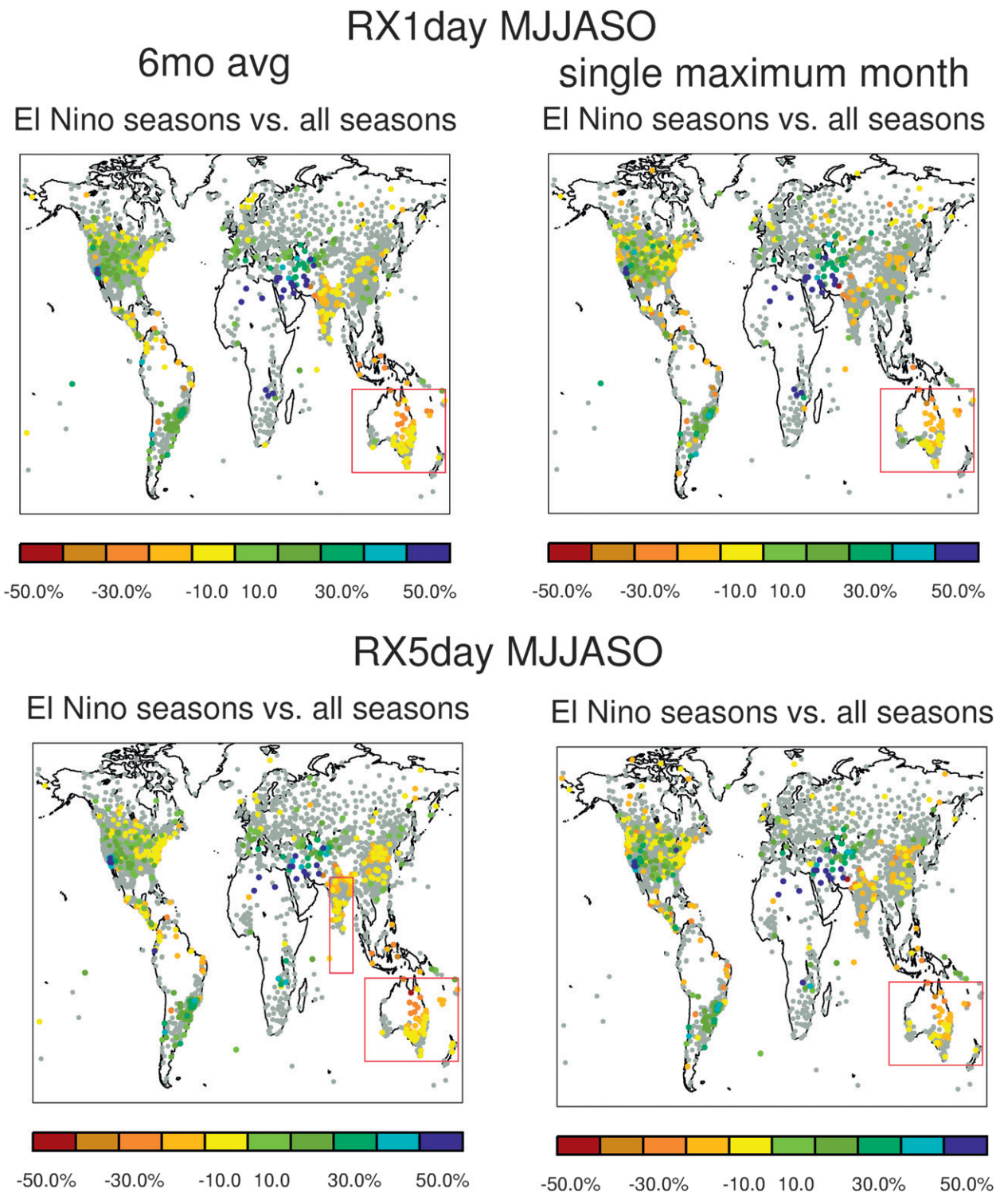

FIG. 4. As in Fig. 2, but showing the boreal summer (MJJASO) response for RX1day (top row) and RX5day (bottom row). Changes are shown for the El Niño phase only. The left-hand panels show the monthly average extreme values, and the right-hand panels show the seasonal extreme value. Fewer regions have 25% or greater stations with a significant response. A range of stations extending from northern Africa through the Middle East shows a significant response in boreal summer, which is not evident during winter (Fig. 2). India experiences a shift from more extreme events in winter to fewer during summer. Results for the La Niña phase are very similar, but opposite in sign.

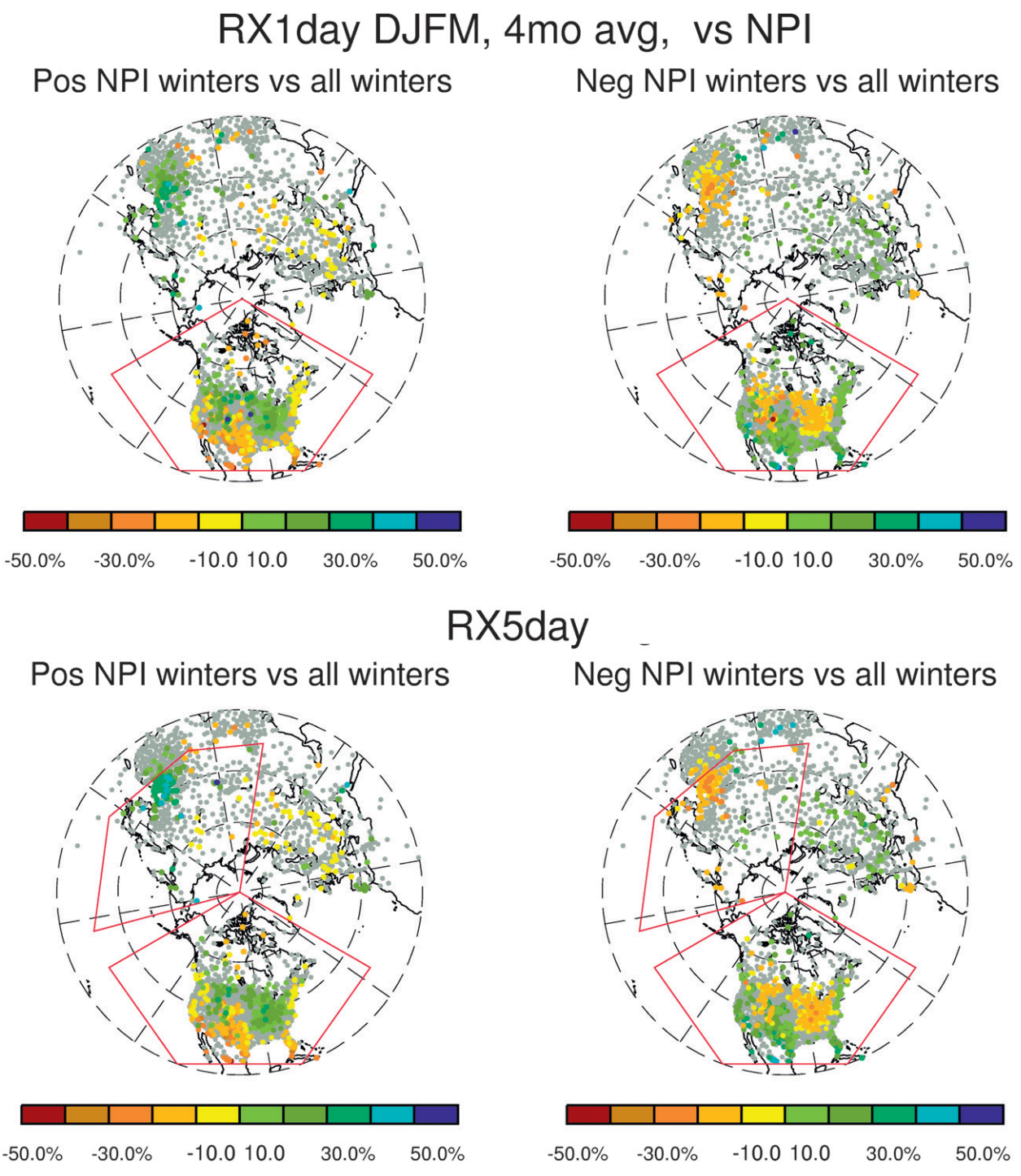

FIG. 5. Difference (%) of extreme precipitation in winter (DJFM) seasons with (left) a positive and (right) negative NPI from the average of all winter seasons for the seasonal average (top) RX1day and (bottom) RX5day indices. Available stations that do not show a significant response are displayed in light gray. Red boxes outline regions where 25% or greater stations responded significantly to NPI phases. The southwest United States and northern Mexico experience a decrease in extreme precipitation during positive NPI, while Idaho, Montana, and the Ohio–Mississippi River valleys respond with a moderate increase.

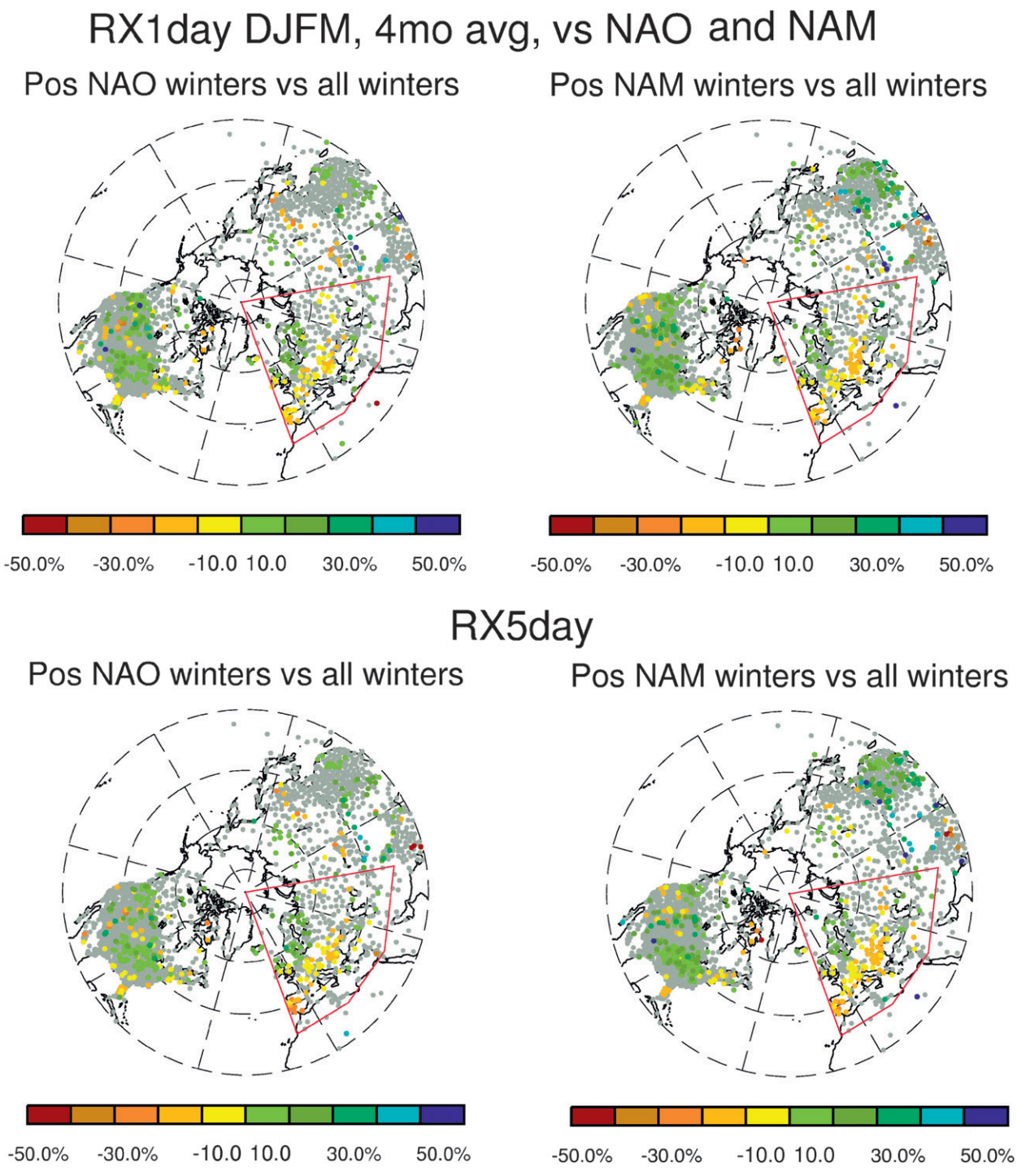

FIG. 6. As in Fig. 5, but for the differences in (left) positive NAO and (right) NAM winter (DJFM) seasons from the average of all winter seasons for the seasonally averaged RX1day (top row) and RX5day (bottom row) indices. Europe is most strongly affected; however, there is also a distinct region of response in central and southeastern Asia, which responds stronger to the NAM. The Iberian Peninsula shows the strongest response with fewer extreme precipitation events during positive NAO, and more during the negative phase. There is a strong response of opposite effect in central Asia, suggesting a dipole response. There is also the opposite effect north of about latitude 50°N where more extreme precipitation events occur during the positive phase. The response in the seasonal most extreme value is very similar but slightly muted and that to negative circulation anomalies is similar, but opposite (not shown).

TABLE 1. Percent of stations with a significant response, at the 5% significance level, to El Niño (i.e., the CTI) for eight regions: North America, South America; Europe (to 70°E); East Asia (30°N, 70°E–90°N, 180°), Africa, India (10°S, 70°E–30°N, 90°E), Southeast Asia (10°S, 90°E–30°N, 180°), and Australia. Shown are seasonally averaged monthly RX1day and RX5day extremes, and single maximum months (in parentheses). The first column shows the instantaneous comparison to CTI. Following columns are results for CTI leading the precipitation index by 1 and 3 months, respectively (ONDJFM or ASONDJ for boreal winter and AMJJAS and FMAMJJ, respectively, for boreal summer). Values ≥20% are italicized, and those ≥30% are set in boldface.

Percent significant stations, ENSO, boreal winter (NDJFMA)						
	RX1day (max) (%)	RX1day 1-month lag (%)	RX1day 3-month lag (%)	RX5day (max) (%)	RX5day 1-month lag (%)	RX5day 3-month lag (%)
N America	*29* (14)	**31** (14)	**30** (14)	**30** (14)	**32** (14)	**32** (14)
S America	15 (14)	16 (15)	17 (14)	*23* (*21*)	*23* (20)	19 (13)
Europe	16 (15)	*20* (14)	*20* (14)	12 (15)	*20* (14)	*23* (15)
East Asia	*29* (12)	**31** (13)	**30** (14)	*29* (13)	*24* (13)	*25* (12)
Africa	*23* (11)	*25* (8)	*25* (8)	*23* (10)	*26* (12)	*27* (12)
India	15 (13)	16 (12)	16 (15)	14 (13)	14 (15)	12 (12)
SE Asia	*27* (13)	*27* (11)	*28* (12)	**30** (14)	**31** (18)	**31** (20)
Australia	*28* (13)	*26* (16)	*29* (15)	**34** (18)	**30** (19)	**30** (16)
Percent significant stations, ENSO, boreal summer (MJJASO)						
	RX1day (max) (%)	RX1day 1-month lag (%)	RX1day 3-month lag (%)	RX5day (max) (%)	RX5day 1-month lag (%)	RX5day 3-month lag (%)
N America	13 (12)	13 (12)	12 (12)	12 (12)	12 (13)	13 (13)
S America	*24* (*21*)	*22* (19)	**40** (*21*)	*23* (*21*)	*23* (*20*)	**48** (**31**)
Europe	*21* (16)	17 (15)	16 (14)	*22* (19)	18 (16)	18 (16)
East Asia	15 (10)	12 (10)	13 (11)	18 (11)	16 (12)	15 (11)
Africa	*23* (17)	*21* (18)	*23* (*21*)	*26* (18)	*21* (*20*)	18 (17)
India	*23* (9)	*24* (11)	17 (11)	*29* (14)	**32** (13)	*26* (15)
SE Asia	10 (9)	9 (9)	9 (9)	15 (14)	13 (12)	9 (13)
Australia	**45** (**35**)	**41** (**31**)	**31** (22)	**47** (**34**)	**40** (*28*)	**36** (*26*)

response is associated with distinct seasonal differences (Figs. 2–4). During the boreal cold season (NDJFMA), the whole southern half of North America, including Mexico and Central America, experiences wetter precipitation extremes during El Niño phases. This is especially true for the Pacific coast, with some stations showing a 50% or more increase in intense precipitation compared to the station's long-term mean (Fig. 2, lhs). Very pronounced changes also occur in India, where some stations on the west coast and in northeastern India display up to a 50% increase in extreme precipitation in the boreal cold season for both the RX1day and RX5day indices. The middle third of North America (as well as the Pacific Northwest) shows slightly or moderately reduced heavy precipitation during cold season El Niños, as does southern Africa and large parts of Australia. The Philippines and Southeast Asia show much reduced heavy precipitation for both the RX1day and RX5day indices. The stations with the most significant changes over the station mean index are also strongly correlated (not shown) to the CTI with peak correlation ranging to ≥0.8 in the southern United States, the south coast of Brazil, NW India, and SE China, and ≤−0.8 in northern South America and the Philippines. Boreal cold season La Niña phases largely bring about the reverse signal from the above (right panels in Figs. 2 and 3). Regions where ≥25% of the stations are responding significantly to a circulation index are outlined by red boxes (the region boundaries, drawn slightly smaller for clear distinction, are described in the caption for Table 1). It is also noticeable, both from Table 1 and Fig. 3, that the number of significant stations reduces substantially when moving from the average precipitation of the wettest day per month to that of the wettest per half-year, with no region showing more than 25% of the stations responding, while the pattern remains very similar (Figs. 2 and 3). This suggests that the sampling variability for more extreme events is substantial.

During the boreal warm season (MJJASO; see Fig. 4) the El Niño–La Niña phases have a weaker effect on North American extreme precipitation than during the cold season, possibly because local convection rather than dynamical systems becomes the driving force for extreme precipitation in summer. The exception is southwestern California and the Baja Peninsula, which respond with markedly wetter RX indices in warm season El Niño phases. The percentage of significant stations also decreases for boreal summer (note the fewer red boxes in the plots). In some regions of the globe, the boreal summer signal is more intense than in the boreal cold season. For instance, we now see some stations in the Sahara and

TABLE 2. As in Table 1, but for annual-only indices. It can be seen that relationships to large-scale circulations degenerate toward indices representing the more extreme events, with PRCPTOT on the left and the most extreme (R99P) on the right. This suggests that the most extreme events are more strongly influenced by local dynamics and random noise than by large-scale circulation patterns. Correlations of annual values are generally, but not always, weaker than seasonal ones in the dynamically active season.

Percent significant stations, ENSO, boreal winter (NDJFMA)					
	PRCPTOT (%)	RX1day (%)	RX5day (%)	R95P (%)	R99P (%)
N America	18	14	12	13	9
S America	*27*	11	14	15	8
Europe	16	8	11	10	5
East Asia	15	8	10	12	6
Africa	17	10	9	12	3
India	*26*	14	*22*	16	5
SE Asia	16	9	9	9	6
Australia	**56**	17	*26*	**32**	12

the Middle East experience a strong (up to 50%) increase in extreme precipitation during El Niño seasons, and the northeast coast of the United States and India now experience reduced extreme precipitation. During the austral cold half-year, northern Australia and Indonesia show strongly reduced intense precipitation during El Niño phases (Fig. 4) but only moderate intensification during La Niña (not shown). We find our MJJASO results to be more similar to the results of Alexander et al. (2009) than those of the NDJFMA season. In contrast to the boreal cold season, the seasonal extreme indices respond almost as strongly as the average of the monthly extremes (cf. the right panels in Fig. 4 to the left panels; see also Table 1).

On the annual scale (not shown), ENSO affects extreme precipitation for all five indices (Table 2). The response of the maximum precipitation indices shows wetter extremes for the annual mean in the mountain west of the United States, and in Brazil–northern Argentina. Australia evidences a much lower chance of extreme precipitation annually during El Niño and a much higher chance during La Niña phases. Likewise, northern India, the Philippines, Southeast Asia, and Central America experience more extreme precipitation during La Niña phases (drier during El Niño; similar to Figs. 2–4). PRCPTOT shows results that are consistent with the changes in extreme precipitation and those described in the literature. The two percentile indices (R99P and R95P) show a reduced chance for extreme precipitation in the same regions where PRCPTOT, RX5, and RX1 are reduced, and a much enhanced chance for extreme precipitation in the southwestern United States, and for a few stations in Chile and southern Brazil (not shown). La Niña phases bring the reverse signal for these indices. Table 2 also illustrates that in transition from average to extreme indices, the number of stations with significant differences between El Niño and La Niña decreases substantially, indicating that random variability begins to dominate over circulation influences for indices of rare extremes.

TABLE 3. As in Table 1, but here the stations are tested for their response to the NPI (for DJFM, as the NPI is considered mainly a winter influence).

	RX1day (max) (%)	RX5day (max) (%)
N America	*27* (16)	*28* (18)
Europe	15 (14)	*20* (12)
East Asia	*24* (14)	*25* (15)

b. NPI

During the positive phase of the NPI the western North Pacific is warm with a weaker Aleutian low, while western Canada and Alaska are colder. The NPI impacts on the extreme precipitation indices are broadly consistent with the response to El Niño, but of opposite sign (see Zhang et al. 1997; Mantua et al. 1997). We confine our analysis of the Pacific decadal variability to the Northern Hemisphere and to the RX indices, since these indices are available monthly and can be constructed into the DJFM winter season.

The impacts on extreme precipitation are strongest in North America (Fig. 5). This reflects the results in Meehl and Hu (2006). More than 25% of the stations in North America respond to the NPI for both RX indices. East Asia also shows a strong response. Central China, the mountain west of the United States, and the Mississippi drainage basin are much wetter during the positive NPI phase. The RX1day index (Fig. 5, top panels) has a slightly weaker reaction than that of RX5day, with more moderate increases in heavy precipitation in China and the mountain west of the United States. The results for both RX indices show a substantial reduction in heavy precipitation in Mexico as well as the southern United States, most noticeably in California, Texas, and Florida. Results of the single-most extreme event per season (not shown) are similar but noisier, with approximately half as many (Table 3) stations around the Pacific Rim reporting significant differences between positive and negative NPI. The percentage of affected stations (Table 3) is similar to those affected by El Niño during the boreal cold season, and, like El Niño, the Pacific interdecadal variability mostly impacts those regions that are close to the regime, and dynamically downstream; consistent with the results in Meehl et al. (2007). Correlations (not shown) of the RX indices to the NPI are strong, especially in southern Japan and in the Ohio–Mississippi River valleys of the United States, where they reach values of 0.7.

TABLE 4. As in Table 3, but here the stations are tested for their response to the NAO, the NAM (middle section), and the SAM (bottom section). Regions shown for the SAM were chosen based on the number of responding stations; hence, Africa, with too few responses, is not shown.

Significant stations, NAO, boreal winter (DJFM)		
	RX1day (max) (%)	RX5day (max) (%)
N America	14 (10)	12 (12)
Europe	*28* (17)	*29* (21)
East Asia	13 (10)	13 (10)
Significant stations, NAM, boreal winter (DJFM)		
	RX1day (max) (%)	RX5day (max) (%)
N America	17 (13)	13 (12)
Europe	*29* (17)	*33* (22)
East Asia	15 (8)	17 (9)
Significant stations, SAM, austral winter (MJJA)		
	RX1day (max) (%)	RX5day (max) (%)
S America	22 (16)	22 (17)
Australia	16 (12)	13 (13)
SE Asia	14 (15)	7 (9)

c. NAO

Figure 6 shows results for the NAO impacts on the RX indices during boreal winter (DJFM). Like the NPI, the NAO is mostly a wintertime phenomenon (e.g., Hurrell et al. 2003). There may be some influence on mean precipitation during other seasons, but as Haylock and Goodess (2004) point out, summer convection and local processes significantly reduce any spatial coherence in extreme precipitation, and would dominate over any signal that might arise from large-scale circulation (see Hurrell et al. 2003). The NAO regime is known to be one of the main influences on European winter weather, and our results show the strongest correlation (correlation coefficients peaking at nearly 0.8) to NAO in Europe and central Asia. In the European region, 28% of the stations show a significant response (Table 4).

As can be seen in Fig. 6, the positive phase of the NAO (see the lhs panels), when the pressure difference between the Icelandic low and the Azores high is anomalously strong, is associated with a strongly reduced chance of extreme precipitation over the Iberian Peninsula and Ireland, and a moderately reduced chance through most of Europe. Meanwhile, consistent with Scaife et al. (2008), Scotland and Scandinavia have increased heavy precipitation during positive phases and decreased heavy precipitation during the negative phases. Interestingly, we also find that some stations much farther east, in western China around the Tibetan Plateau, experience strongly reduced extreme precipitation events during positive NAO years, and we find about 10% of stations responding in North America at the 5% significance level, with particularly the Pacific Northwest region showing more intense precipitation extremes. In contrast, Zhang et al. (2010) did not find a convincing influence of the NAO on North American extreme winter precipitation, with only 6% of stations showing a significant response. Negative NAO winters show a similar response but of opposite sign (not shown). Results using just the single maximum over the entire season (not shown) are similar but not nearly as strong (see also Table 4). This suggests similar mechanisms for heavy and very heavy precipitation, but that sampling noise becomes more of an issue when going farther out the tail of the distribution.

To investigate if this hemisphere-wide response is more reflective of the hemispheric-wide NAM, we used the NAM index for comparison (Fig. 6, right panel). The results are very similar, but generally slightly stronger (Table 4) and support an almost zonal response of precipitation extremes with the NAO–NAM. There is now also a stronger response in Southeast Asia.

Gillett et al. (2006) show a clear response of Southern Hemispheric midlatitude mean precipitation to the Southern Annular Mode (SAM). However, we find only a very weak response of precipitation extremes in the few regions that are covered by extremes indices (Table 4; not shown), and the result was sensitive to subtracting the trend in the SAM.

5. Conclusions

Five indices of extreme precipitation for hundreds of stations across the globe were analyzed against the positive and negative phases of large-scale circulation modes. The large-scale circulations investigated were the ENSO-like SST patterns represented by the cold tongue index (CTI; note that we use a more generous definition of positive–negative events than the dynamical El Niño–La Niña condition), NAO, NAM, SAM, and Pacific interdecadal variability as represented by the North Pacific index (NPI). The extreme indices analyzed were RX1day and the wettest 5-day event, RX5day. We also explored the annual total precipitation (PRCPTOT) and the percent of days exceeding the climatological 95th and 99th percentiles.

The relationship between the indices at each station and the circulation modes were analyzed using a Mann–Whitney test. Stations with a response at the 5% significance level were spread across the globe and often display regional coherence in their response, showing that the large-scale circulations have global-scale teleconnection effects. This widespread response was observed for all indices, but Pacific interdecadal variability has its strongest

influence around the landmasses adjacent with the Pacific (including all of the United States), while the NAO influence appears strongest in Eurasia. The response of the precipitation extremes to circulation was most clear for the winter hemisphere, which is understandable if, during summer months, dynamic forcings diminish and local convection takes over; and response patterns of extreme precipitation to circulation are distinctly different between the boreal cold and warm seasons, particularly in India, Africa, Australia, East Asia, and the northern United States.

The three annual indices (R99P, R95P, and PRCPTOT) responded with wetter extremes in the SW United States and Brazil during El Niño phases, and reduced extremes in Central America, northern India, China, the Philippines, and Australia.

The NPI and NAO are largely relevant for the months of DJFM and particularly affect North America and East Asia. The response to the NPI circulation index for East Asia shows stronger wet extremes for positive NPI and reduced extremes for negative NPI. North America shows a heterogeneous response to the phases of the NPI in which the Pacific coast, southwest United States, Texas, the high plains, and Florida exhibit strongly reduced heavy precipitation during positive phases of the NPI, while the Mountain West and the Ohio–Mississippi basin (excluding the Gulf coast) show intensified heavy precipitation.

The response of the RX indices to the NAO is strong in Eurasia. South of approximately 55°N, heavy precipitation is reduced in positive phases of the NAO and increased, especially in the Iberian Peninsula, in negative phases. Above the approximate line at 55°N, the opposite conditions prevail with wetter conditions during positive NAO and a drier pattern during negative NAO, which appears to extend as far east as the Tibetan Plateau. This response, together with a weaker response in North America, is better explained by the Northern Annular Mode than the Atlantic sector NAO.

Those stations for which precipitation extremes respond to circulation indices show similar correlations to circulation as were earlier found for temperature extremes (KH08). However, fewer stations overall responded, indicating that for precipitation the local effects (and/or noise) outweigh the effects from large-scale dynamics, especially during the summertime. This reduction in the number of responding stations may be partly due to the stronger spatial inhomogeneity of precipitation compared to temperature. Precipitation also generally has a smaller spatial autocorrelation than temperature, particularly during convective times of the year or in regions where convection dominates over dynamic causes of precipitation.

We find significant precipitation responses largely in the same regions as temperature responses, with the exception that precipitation responses do not extend as far into the high latitudes, consistent with earlier observations for total precipitation (Ropelewski and Halpert 1986). We also find a strong ENSO response in the precipitation extremes in the Sahara and the Arabian Peninsula that was not seen in the temperature study.

In conclusion, precipitation extremes respond to circulation globally, with seasonally varying signatures. These responses are similar to those reported for total precipitation and weaken slightly when going farther out into the tail of the precipitation distribution.

Acknowledgments. We thank Lisa Alexander for providing the extremes indices, Clara Deser for suggesting and providing the NPI index, and Jerry Meehl and a second, anonymous, reviewer for their insightful and constructive suggestions. We also thank Alex Robel for analysis of some station records and the suggestion to investigate lags. The authors were supported by NSF Grant ATM-0296007, NOAA Grant NA16GP2683, Edinburgh University, and Duke University.

REFERENCES

Alexander, L. V., and Coauthors, 2006: Global observed changes in daily climate extremes of temperature and precipitation. *J. Geophys. Res.,* **111,** D05109, doi:10.1029/2005JD006290.

——, P. Uotila, and N. Nicholls, 2009: The influence of sea surface temperature variability on global temperature and precipitation extremes. *J. Geophys. Res.,* **114,** D18116, doi:10.1029/2009JD012301.

Allan, R. P., and B. J. Soden, 2008: Atmospheric warming and the amplification of precipitation extremes. *Science,* **321,** 1481–1484.

Arblaster, J. M., G. A. Meehl, and A. Moore, 2002: Interdecadal modulation of Australian rainfall. *Climate Dyn.,* **18,** 519–531.

Deser, C., A. S. Phillips, and J. W. Hurrell, 2004: Pacific interdecadal climate variability: Linkages between the tropics and the North Pacific during boreal winter since 1900. *J. Climate,* **17,** 3109–3124.

Frich, P., L. Alexander, P. Della-Marta, B. Gleason, M. Haylock, A. M. G. Klein Tank, and T. Peterson, 2002: Observed coherent changes in climatic extremes during the second half of the twentieth century. *Climate Res.,* **19,** 193–212.

Gillett, N. P., T. D. Kell, and P. D. Jones, 2006: Regional climate impacts of the Southern Annular Mode. *Geophys. Res. Lett.,* **33,** L23704, doi:10.1029/2006/GL027721.

Groisman, P., R. Knight, D. R. Easterling, T. R. Karl, G. Hegerl, and Vy. N. Razuvaev, 2005: Trends in intense precipitation in the climate record. *J. Climate,* **18,** 1326–1350.

Haylock, M., and C. M. Goodess, 2004: Interannual variability of European extreme winter rainfall and links with mean large-scale circulation. *Int. J. Climatol.,* **24,** 749–776.

Hegerl, G. C., and J. M. Wallace, 2002: Influence of patterns of climate variability on the difference between satellite and surface temperature trends. *J. Climate,* **15,** 2412–2428.

——, F. Zwiers, S. Kharin, and P. Stott, 2004: Detectability of anthropogenic changes in temperature and precipitation extremes. *J. Climate,* **17,** 3683–3700.

Hurrell, J. W., and H. van Loon, 1997: Decadel variations in climate associated with the North Atlantic Oscillation. *Climatic Change,* **36,** 301–326.

——, Y. Kushnir, G. Ottersen, and M. Visbeck, 2003: An overview of the North Atlantic Oscillation. *The North Atlantic Oscillation: Climate Significance and Environmental Impact,* J. W. Hurrell et al., Eds., Amer. Geophys. Union, 1–36.

Kenyon, J., and G. C. Hegerl, 2008: Influence of modes of climate variability on global temperature extremes. *J. Climate,* **21,** 3872–3889.

Mantua, N. J., S. R. Hare, Y. Zhang, J. M. Wallace, and R. C. Francis, 1997: A Pacific interdecadal climate oscillation with impacts on salmon production. *Bull. Amer. Meteor. Soc.,* **78,** 1069–1079.

McGregor, S., N. J. Holbrook, and S. B. Power, 2007: Interdecadal sea surface temperature variability in the equatorial Pacific Ocean. Part I: The role of off-equatorial wind stresses and oceanic Rossby waves. *J. Climate,* **20,** 2643–2658.

——, ——, and ——, 2008: Interdecadal sea surface temperature variability in the equatorial Pacific Ocean. Part II: The role of equatorial–off-equatorial wind stresses in a hybrid coupled model. *J. Climate,* **21,** 4242–4256.

Meehl, G. A., and A. Hu, 2006: Megadroughts in the Indian monsoon region and southwest North America and a mechanism for associated multidecadal Pacific sea surface temperature anomalies. *J. Climate,* **19,** 1605–1623.

——, C. Tebaldi, H. Teng, and T. C. Peterson, 2007: Current and future U.S. weather extremes and El Niño. *Geophys. Res. Lett.,* **34,** L20704, doi:10.1029/2007GL031027.

Peterson, T. C., and M. J. Manton, 2008: Monitoring changes in climate extremes. *Bull. Amer. Meteor. Soc.,* **89,** 1266–1271.

Power, S., T. Casey, C. Folland, A. Colman, and V. Mehta, 1999: Interdecadal modulation of the impact of ENSO on Australia. *Climate Dyn.,* **15,** 319–324.

——, M. Haylock, R. Colman, and X. Wang, 2006: The predictability of interdecadal changes in ENSO activity and ENSO teleconnections. *J. Climate,* **19,** 4755–4771.

Rasmusson, E. M., and T. H. Carpenter, 1982: Variations in tropical sea surface temperature and surface wind fields associated with the Southern Oscillation/El Niño. *Mon. Wea. Rev.,* **110,** 354–384.

——, and J. M. Wallace, 1983: Meteorological aspects of the El Niño/Southern Oscillation. *Science,* **222,** 1195–1202, doi:10.1126/science.222.4629.1195.

Ropelewski, C. F., and M. S. Halpert, 1986: North American precipitation and temperature patterns associated with the El Niño/Southern Oscillation (ENSO). *Mon. Wea. Rev.,* **114,** 2352–2362.

Scaife, A. A., C. K. Folland, L. V. Alexander, A. Moberg, and J. D. Knight, 2008: European climate extremes and the North Atlantic Oscillation. *J. Climate,* **21,** 72–83.

Soden, B. J., D. L. Jackson, V. Ramaswamy, M. D. Schwarzkopf, and X. Huang, 2005: The radiative signature of upper tropospheric moistening. *Science,* **310,** 841, doi:10.1126/science.1115602.

Thompson, D. W. J., and J. M. Wallace, 1998: The Arctic Oscillation signature in the wintertime geopotential height and temperature fields. *Geophys. Res. Lett.,* **25,** 1297–1300.

——, and ——, 2001: Regional climate impacts of the Northern Hemisphere Annular Mode. *Science,* **293,** 85–89.

——, ——, and G. C. Hegerl, 2000: Annular modes in the extratropical circulation. Part II: Trends. *J. Climate,* **13,** 1018–1036.

Trenberth, K. E., and J. W. Hurrell, 1994: Decadal atmospheric–oceanic variations in the Pacific. *Climate Dyn.,* **9,** 303–319.

von Storch, H., and F. W. Zwiers, 1999: *Statistical Analysis in Climate Research*. Cambridge University Press, 484 pp.

Wentz, F. J., L. Ricciardulli, K. Hilburn, and C. Mears, 2007: How much more rain will global warming bring? *Science,* **317,** 233, doi:10.1126/science.1140746.

Zhang, X., J. Wang, F. W. Zwiers, and P. Ya. Groisman, 2010: The influence of large-scale climate variability on winter maximum daily precipitation over North America. *J. Climate,* **23,** 2902–2915.

Zhang, Y., J. M. Wallace, and D. S. Battisti, 1997: ENSO-like interdecadal variability: 1900–93. *J. Climate,* **10,** 1004–1020.